Cell structure destruction and its kinetics during hydrothermal treatment of sewage sludge

Apip Amrullah*,**, Nattacha Paksung*, and Yukihiko Matsumura*,†

*Department of Mechanical Sciences and Engineering, Hiroshima University, Higashi-Hiroshima, Japan
**Original Affiliation: Department of Mechanical Engineering, Lambung Mangkurat University,
Banjarmasin, South Kalimantan, Indonesia

Abstract−During hydrothermal treatment (HT) of sewage sludge (SS), its cell structure is decomposed and its organic content is released. An increase in the total organic carbon content in the liquid phase was experimentally determined in the temperature range of 130-250 °C with a fixed pressure of 5 MPa and residence time of 10 min. By using the Arrhenius equation, the pre-exponential factor and activation energy were successfully determined for the first time for the degradation of SS cells as 3.96×10^{10} s^{-1} and 115 kJ mol^{-1}, respectively, for the temperature range of 130-250 °C. Increasing the HT temperature increasingly destroyed the cell structure of SS.

Keywords: Hydrothermal Treatment, Sewage Sludge, Total Organic Carbon, Cell Structure

INTRODUCTION

Sewage sludge (SS), which is the by-product of wastewater treatment, is mainly composed of micro-organisms generated in excess during waste water treatment. With rising urban populations and demand for better treatment of effluent, there has been a large increase in sludge generation [1-4]. However, the treatment and disposal of SS presents a number of environmental challenges [5-7]. The current practices of SS treatment and removal include disposing of treated sludge to agricultural land, [8] incinerating it, [9] or discarding it in landfills [10]. A variety of approaches have been employed to improve the SS dewaterability, such as thermal treatment which is pyrolysis [11,12], combustion, and supercritical water gasification [13-18], ultrasonication [19], freezing and thawing [20].

Recently, hydrothermal treatment (HT) has been introduced as an emerging dehydration technology to reduce the moisture content of SS and improve its dewaterability [21]. Qiao et al. [9] and Urrea et al. [22] reported that HT could disrupt the sludge cell structure and release bound water to improve sludge dewaterability and easier handling. HT is also known as an effective pretreatment for biomethanation, as demonstrated by Haug et al. [23], who reported that thermal treatment of sludge before anaerobic digestion led to increased biodegradability and dewaterability.

Hence, HT is a promising method for processing SS as it results in the formation of a stable and sanitized product [24-26]. The HT process employs high pressure to convert waste into useable products and it does not require dry feedstock, making it suitable for wet biomass such as SS [27,28].

Previous studies have investigated the utility and application of HT technology. Kato and Matsumura [29] investigated HT as a

means to ease biomass slurry delivery. Matsumoto et al. [30] investigated the effect of salts on the hydrothermal pretreatment of kelp. Here, more than 80% of the total organic carbon (TOC) moved into the liquid phase, leaving only ~10% in the solid phase. Recently, Yin et al. [31] attempted a detailed kinetics model for HT of sewage sludge based on an explicit reaction including protein, saccharide, NH$_4^+$-N and acetic acid using batch test conditions. Moon et al. [32] investigated the HT of SS and showed that it could help enhance the quality of the product gas while also reducing the moisture content of the sludge. Additionally, Yoshida et al. [33] studied the HT of cellulose as a pretreatment for ethanol fermentation. They developed a reaction kinetics scheme for the hydrolysis of cellulose to glucose in order to identify optimal HT conditions. Finally, Petchpradab et al. [34] investigated hydrothermal pretreatment of rubber wood for the saccharification process. They proposed a reaction network model for this pretreatment step and applied it successfully.

Meanwhile, the ability to change the cell structure of SS by HT is urgently needed. Yu et al. [35] reported that the dewaterability of activated sludge first deteriorated but then ameliorated when the temperature was raised from 100 °C to 200 °C, with a threshold temperature of 130 °C, under hydrothermal conditions. Kyotani et al. [36] reported that the morphological characteristics of sludge flocs had a relatively weak impact on their dewaterability. Wang et al. [37] also determined the HT is an effective method to enhance the deep dewaterability of excess sludge with low energy consumption.

Overall, the phenomena observed by HT of SS can be summarized as follows. The cell structure of SS begins to degrade when it is heated in pressurized water, which releases organic matter from the cell structure, leading to an increase of the organic content in the liquid phase. Further temperature increases or longer treatment times result in hydrothermal carbonization or direct liquefaction [38,39], which leads to larger amounts of organic compounds in the liquid phase. Together with the progression of the HT process, the slurry viscosity is decreased, its dewaterability is improved, and the

---

†To whom correspondence should be addressed.
E-mail: mat@hiroshima-u.ac.jp

fermentation rate is improved.

Despite numerous studies on the effect of HT on the characteristics of SS, to the best of our knowledge, there have been no comprehensive studies on the morphological structure of sewage or the release of its inner cell compounds by HT. Kinetics studies have been conducted for hydrothermal carbonization only, and the degradation rate of the cell structure has not been elucidated. Therefore, we investigated the effect of HT at various temperatures (130-250 °C) on the morphological structure of SS as well as the release of organic compounds inside the cells and its kinetics behavior.

MATERIAL AND METHODS

1. Material

The SS used as the feedstock for the HT process was active sludge collected from a wastewater treatment plant center in Higashi-Hiroshima, Japan. Active sludge consists of a mixed community of microorganisms, approximately 95% bacteria and 5% higher organisms (i.e., protozoa, rotifers, and higher forms of invertebrates) [40]. After collection, the sludge was filtered by suction filtration with filter paper (11.0 cm, Whatman Grade 5 Qualitative) and dried (80 °C, until constant weight). It was then pulverized in a ball mill and sieved with a sieve having a mesh size of 40 μm. This treatment was needed for precise concentration and pulverization. Table 1 shows the elemental analysis of the active sludge, as conducted previously by Unami et al. [41].

2. Experimental

A schematic representation of the experimental apparatus is shown in Fig. 1. SS was hydrothermally treated in a continuous

Table 1. Proximate and ultimate analysis of sewage sludge

Water content (%)	Proximate analysis (wt/wt dry base)			Ultimate analysis (wt/wt dry base)				
	VM	FC	Ash	C	H	N	S	O
79.16	77.5	5.83	16.67	43.1	6.60	4.42	2.36	25.9

VM: volatile matter; FC: fixed carbon; C: Carbon; H: hydrogen; N: nitrogen; S: Sulphur; O: oxygen

reactor comprising SS316 steel tubing with a length of approximately 15.7 m and an inner diameter of 4.35 mm. Initially, water was fed into the reactor prior to the experiments. Subsequently, the pressure was adjusted and maintained at 5 MPa using a back-pressure regulator. After achieving a constant pressure of 5 MPa, the reactor temperature was set at the desired temperature. Then, the feedstock slurry (solid concentration: 0.2 wt%) in the pump was pushed out of the cylinder (P-1), by sending water from the other side of the piston, and delivered to the reactor. The pump was produced by NS company (NP-GXL-400). The reactor effluent was then cooled by a heat exchanger (HX). The reaction temperature (130, 150, 180, 210, and 250 °C) was controlled with a furnace. The reaction pressure and residence time were set at 5 MPa and 10 min, respectively, for all experimental runs. The corresponding flow rate of water was 20 mL/min. Table 2 provides a summary of the experimental conditions employed in this study. The liquid containing the solid product was collected from the cylinders (P-2 and P-3).

3. Analytical Method

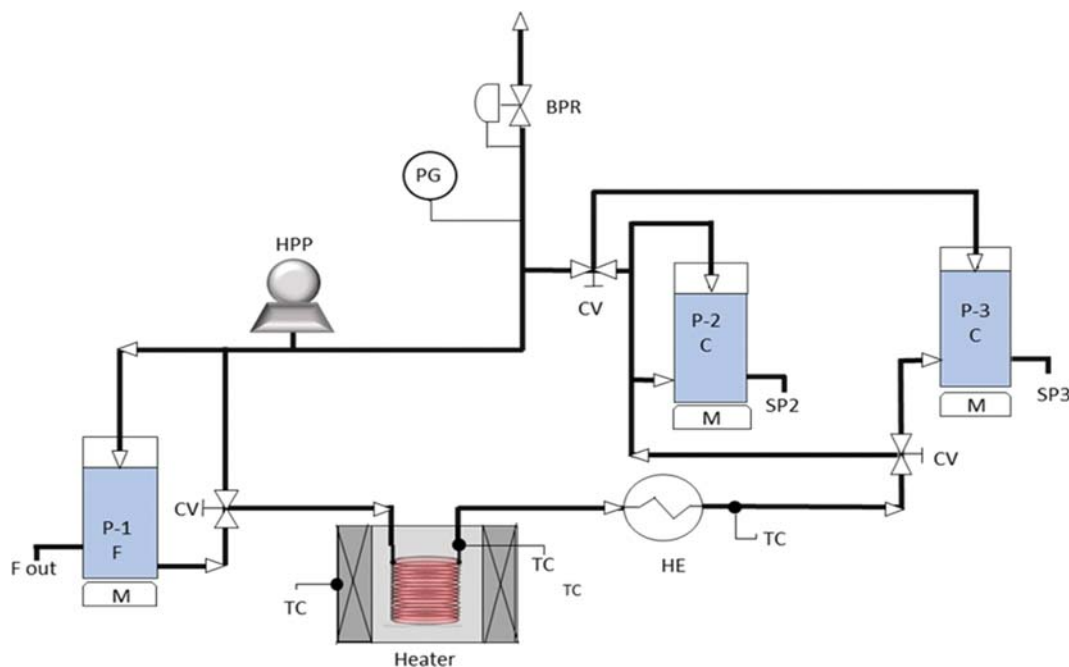The product from the HT process was filtrated to separate the

Fig. 1. Experimental apparatus.

TC. Thermocouple	BPR. Back pressure regulator	SP2, SP3. Sampling port 2 and 3
HE. Heat exchanger	CV. Check valve	M. Magnetic stirrer
HPP. High pressure pump	P-1F. Piston pump feedstock	
PG. Pressure gauge	P-2C, P-3C. Piston pump for collecting sample 2 and 3	

Table 2. Experimental condition

Types of conditions	Experimental range
Feedstock	Sewage sludge
Concentration of solid	0.2 wt%
Temperature	130, 150, 180, 210 and 250 $^\circ$C
Pressure	5 MPa
Residence time	10 min
Flow rate	20 ml/min
Reactor type	Flow reactor

*All experiments were run in duplicate

solid products using filter paper with a size of 11.0 cm (Whatman Grade 5 Qualitative). The liquid sample was analyzed for total organic carbon (TOC) to quantify the amount of carbon in the liquid product (non-purgeable organic carbon, NPOC) and that in the dissolved gas product (inorganic carbon, IC). The amount of this TOC was divided by the carbon amount in the feedstock to calculate the TOC yield. The solid product was observed using a ZEN microscope 2.3 blue edition. The microscope magnifies in two steps by way of the objective and eyepiece lenses, with the magnification being determined by multiplying the objective magnification and eyepiece magnification. In this work, the objective LD A-Plan 40×/0.55 Ph1 and magnification 40× were used. All experimental runs were conducted in duplicate.

RESULTS AND DISCUSSION

1. Effect of HT Temperature on Total Organic Carbon in the Liquid Product

Fig. 2(a) shows the TOC yield in the liquid product for each temperature. Note that the data at 0 $^\circ$C refer to the original feedstock value and the experimental results are reproducible. As seen, the TOC increases with temperature, especially at temperatures higher than 150 $^\circ$C. Further, we note that without HT, the TOC value is non-zero because of pulverization. That is, a fraction of the cells should have been destroyed and their contents released in the liquid phase without HT. Increasing the temperature beyond 150 $^\circ$C resulted in the destruction of the remaining intact cells, and further increased TOC with the temperature. Above 200 $^\circ$C, the increase in the TOC yield ceased, which was likely caused by the complete destruction of the cells. The corresponding TOC yield was 0.162 mol/mol. This result implies that SS cells are composed of water-soluble organic and insoluble organic materials. The latter likely includes cell wall components, and it occupies 0.838 mol-C/mol-C of total organics.

The process temperature has a strong influence on the TOC yield in the liquid phase. For this reason, cell destruction in SS following HT may be satisfactorily treated as a type of reaction that follows Arrhenius' law. This is particularly reasonable since decomposition of the cell structure is caused by thermal decomposition of the cell membrane.

The observations of the present study are consistent with the results of Everett, (1972), who found that the destruction of the cell walls during heat treatment released the cell content and that insolu-
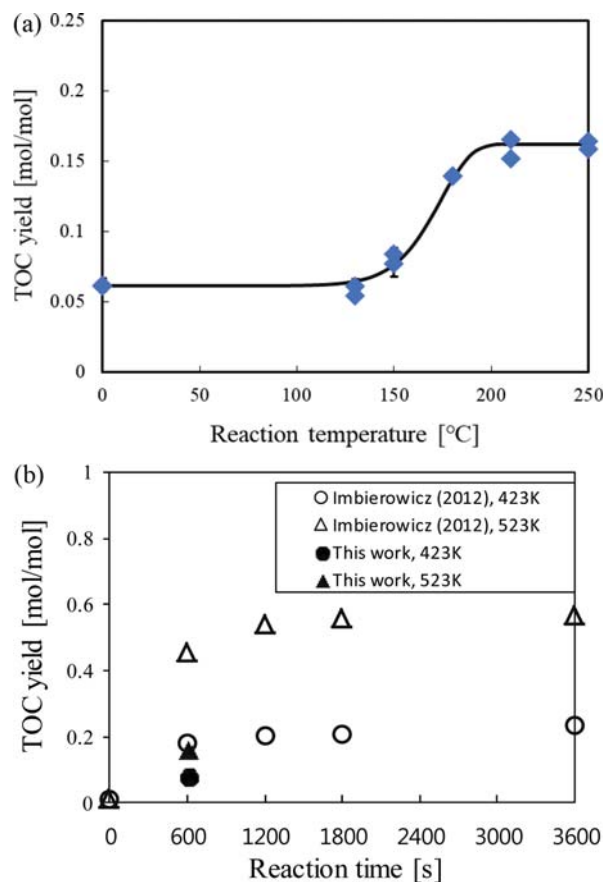

Fig. 2. TOC yields. (a) Effect of temperature on TOC yield. (b) Comparison of TOC yields (experiment conditions: 423 and 523 K, and 600 s).

ble protein was broken down into more soluble compounds (e.g., amino acids). The observations are also consistent with the previous work of Wang et al. [43], who observed that the characteristics of sludge particles such as surface charge and hydrophobicity were improved following HT, and that the bound water in the sludge flocs was released to the bulk water. Imbierowicz et al. [44] reported that the process temperature had a decisive impact on the rate of TOC solid conversion into the liquid phase. Indeed, approximately 50-55% of the initial TOC solid was transferred into the liquid phase. Fig. 2(b) shows a comparison of the present results with those of Imbierowicz et al. As seen, the TOC yield reported herein is significantly lower, especially at 150 and 250 $^\circ$C (423 and 523 K), than that reported previously. This difference may be partly caused by the type of reactor used in each study. This study employed a continuous reactor, whereas Imbierowicz et al. used a batch reactor. Batch reactors usually require relatively longer times for heating and cooling, during which time the reaction proceeds. In this regard, the treatment time employed by Imbierowicz et al. was much longer than that used herein. However, their purpose was to convert the solid fraction into liquid organics, and they even observed a gas product. By comparison, we are more interested in the release of organics following cell destruction.

2. Determination of Reaction Rate Parameters

By assuming a first-order rate equation, the reaction rate con-

stant of TOC release, or destruction of the SS cells, during HT could be determined. For many cases, first-order reactions are found to be effective for such processes. For example, Mohamad et al. [45] used first-order reaction kinetics to determine the rate constant of decomposition of mannitol and sorbitol under hydrothermal condition. They employed the least squares method to determine the reaction parameters, and their first-order reaction model fit the data well. Determining such reaction kinetics is important for designing an appropriate HT reactor for SS. The model can be expressed by the following equation, which expresses the change of carbon:

$$C_{SS} \rightarrow vC_{TOC} + (1-v)C_{Sol} \tag{1}$$

The subscripts SS, TOC, and Sol indicate the original cell, liquid phase, and remaining solid, respectively, and v is the fraction of carbon that is converted into TOC carbon. As shown in Fig. 2(a), all of the cells are destroyed at 250 °C. The TOC yield at this temperature should correspond to the value of v, which is 0.162 mol/mol. Assuming a first-order reaction, the following differential rate equation can be written:

$$\frac{d[C_{SS}]}{dt} = -k[C_{SS}] \tag{2}$$

Here, $[C_{SS}]$ is the concentration of C_{SS}. Mass balance gives:

$$[C_{SS}] + [C_{TOC}] + [C_{Sol}] = const = [C_{SS}]_i + [C_{TOC}]_i + [C_{Sol}]_i = [C_{SS}]_t \tag{3}$$

where the subscript i indicates the initial condition and the subscript t indicates the total amount of SS. It is also noted that:

$$[C_{Sol}] = \frac{1-v}{v}[C_{TOC}] \tag{4}$$

Thus,

$$[C_{SS}] = [C_{SS}]_t - [C_{TOC}] - [C_{Sol}] = [C_{SS}]_t - [C_{TOC}] - \frac{1-v}{v}[C_{TOC}]$$
$$= [C_{SS}]_t - \left(1 + \frac{1-v}{v}\right)[C_{TOC}] = [C_{SS}]_t - \frac{1}{v}[C_{TOC}] \tag{5}$$

Substitution of Eq. (5) into Eq. (2) gives:

$$\frac{d}{dt}\left([C_{SS}]_t - \frac{1}{v}[C_{TOC}]\right) = -k\left([C_{SS}]_t - \frac{1}{v}[C_{TOC}]\right) \tag{6}$$

Namely,

$$\frac{d}{dt}([C_{TOC}]) = vk\left([C_{SS}]_t - \frac{1}{v}[C_{TOC}]\right) \tag{7}$$

$$\frac{d}{dt}\left(\frac{[C_{TOC}]}{[C_{SS}]_t}\right) = vk - k\frac{[C_{TOC}]}{[C_{SS}]_t} \tag{8}$$

Noting that the TOC yield is expressed as:

$$Y_{TOC} = \frac{[C_{TOC}]}{[C_{SS}]_t}, \tag{9}$$

Eq. (8) can be expressed as:

$$\frac{d}{dt}Y_{TOC} = vk - kY_{TOC} \tag{10}$$

This equation can be solved as follows:

$$\frac{dY_{TOC}}{vk - KY_{TOC}} = dt \tag{11}$$

$$\ln(v - Y_{TOC}) = -kt + C \tag{12}$$

$$Y_{TOC} = v - A\exp(-kt) \tag{13}$$

At t=0, the TOC yield is $Y_{TOC,i}$:

$$Y_{TOC} = v - (v - Y_{TOC,i})\exp(-kt) \tag{14}$$

Assuming Arrhenius behavior, the equation for this reaction rate constant is:

$$k = k_0\exp\left(\frac{-E_a}{RT}\right) \tag{15}$$

where k_0, E_a, R, and T are the pre-exponential factor, activation energy, gas constant, and absolute temperature, respectively.

$$Y_{TOC} = v - (v - Y_{TOC,i})\exp\left(-k_0\exp\left(\frac{-E_a}{RT}\right)t\right) \tag{16}$$

The values of the pre-exponential factor and activation energy were determined to reproduce the experimental data using the least squares method. In this way, the pre-exponential factor and activation energy were determined as 3.96×10^{10} s^{-1} and 115 kJ mol^{-1}, respectively.

The calculated TOC yield is shown in Fig. 2(a). As seen, good agreement between the calculated and experimental values is obtained. Fig. 3 shows a parity plot comparing the experimental and calculated data with the model employing the least square error (LSE) method. The high coefficient of determination (R^2) confirms that the model provides a good fit to the experimental data.

Goto et al. [46] determined the activation energies of SS and distillery wastewater decomposition in supercritical water oxidation using a batch reactor. Their values were 76.3 and 64.7 kJ mol^{-1} for SS and distillery wastewater, respectively. Clearly, the activation energy for oxidation is lower than that for HT determined herein (i.e., 115 kJ mol^{-1}).

3. Effect of HT Temperature on the Morphological Structure of Sewage Sludge

The effect of HT on the morphological structure of sewage sludge is shown in Fig. 4, which compares observation of the original
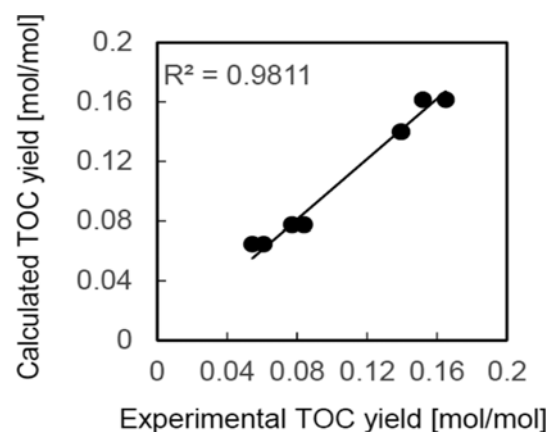

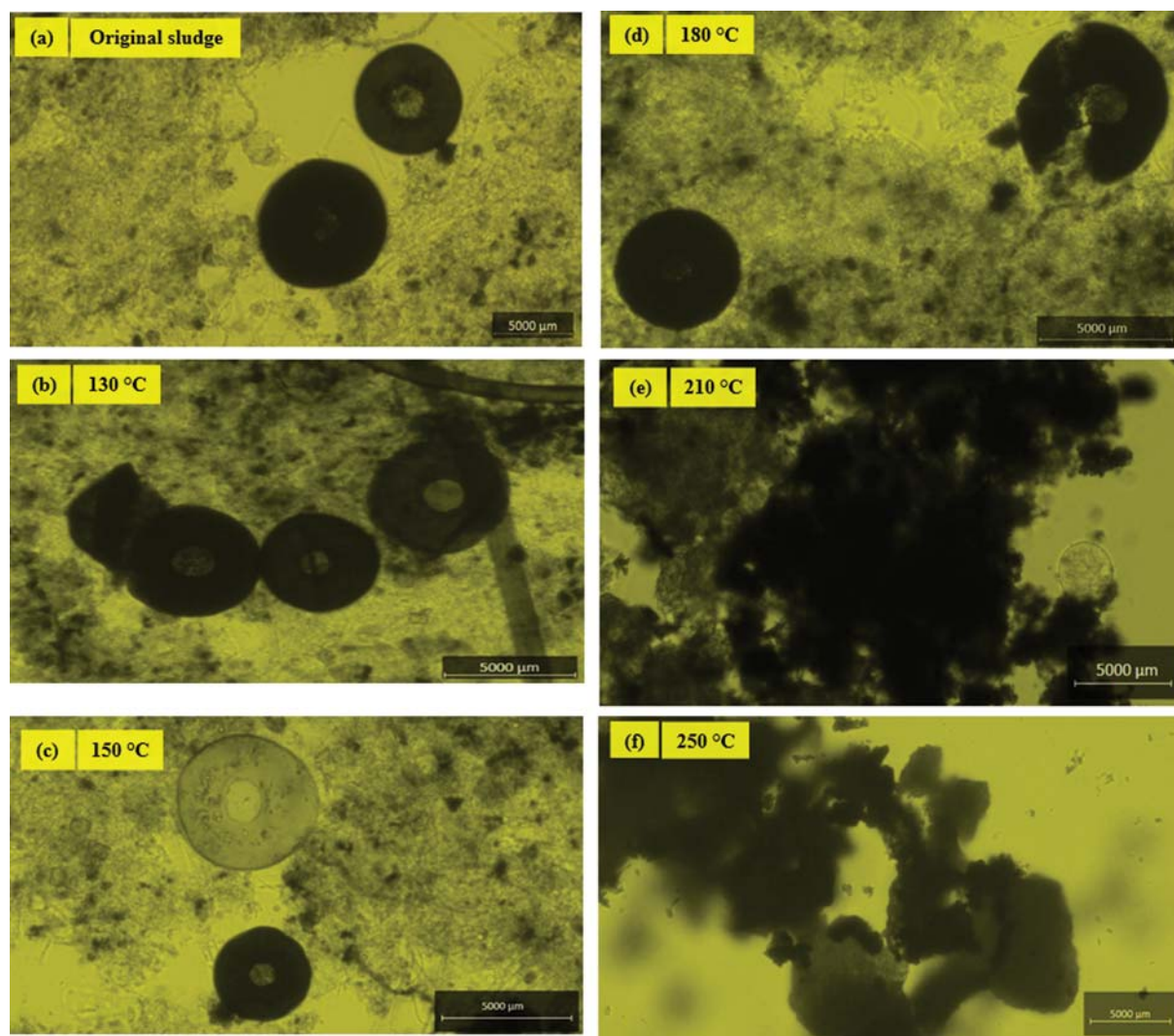Fig. 3. Comparison of experimental and calculated TOC yield.

Fig. 4. Effect of HT temperature on morphology structure of active sludge at (a) Original, (b) 130 °C, (c) 150 °C, (d) 180 °C, (e) 210 °C, and (f) 250 °C.

sludge to that after HT. Consistent with the TOC analysis, it is clear that temperature has a significant impact on the morphological structure of sewage sludge. The original sludge cells are sturdy and wrapped in the fibrous matter, as shown in Fig. 4(a). After HT at 130-150 °C, however, the color of the cells begins to fade (Fig. 4(b) and 4(c)) and some cells appear deformed. At 180 °C, the morphology of the sewage sludge starts to degrade, as clearly seen in Fig. 4(d). The cells are completely destroyed at 210 and 250 °C (Fig. 4(e) and 4(f)). Notably, the cellular changes correspond to the TOC increase in the liquid product at these temperatures (130-250 °C). Imbierowicz and Chacuk [44] observed that the concentration of TOC increased rapidly at 250 °C (523 K) after 20 min. As noted, their reaction includes the conversion of solid compounds into a liquid product, which differs from the present study, where cell degradation and the release of organic material are examined. In another study, Bougrier et al. [47] reported that the thermal treatment modified the characteristics of sludge, including its viscosity and settleability. In that case, the sludge volume index decreased from 140 mg dm^{-3} for untreated sludge to 40 mg dm^{-3} for sludge thermally treated at

170 °C (443 K). Considering the temperature range of their study, this effect on sludge characteristics may well have been caused by cell decomposition.

CONCLUSION

The effect of HT temperature (130-250 °C) on the TOC and morphology of SS was investigated for a residence time of 10 min under 5 MPa. HT damaged the SS cell structure, thereby releasing the cell content and consequently increasing the TOC in the liquid phase. The cell destruction rate was expressed using a first-order rate equation, with the Arrhenius type reaction rate constant. The pre-exponential factor and activation energies for this rate were determined as 3.96×10^{10} s^{-1} and 115 kJ mol^{-1}, respectively. This is the first rate parameters to be reported for the destruction of SS cells.

ACKNOWLEDGEMENTS

REFERENCES

1. R. Li, Z. Ma, T. Yang, B. Li, L. Wei and Y. Sun, *J. Supercrit. Fluids*, **138**, 115 (2018).

2. O. Suárez-Iglesias, J. L. Urrea, P. Oulego, S. Collado and M. Díaz, *Sci. Total Environ.*, **584-585**, 921 (2017).

3. M. S. Nawaz and M. Ahsan, *Alexandria Eng. J.*, **53**, 717 (2014).

4. X. Li, S. Guo, Y. Peng, Y. He, S. Wang, L. Li and M. Zhao, *Biochem. Eng. J.*, **139**, 139 (2018).

5. L. Sahlström, A. Aspan, E. Bagge, M. L. Danielsson-Tham and A. Albihn, *Water Res.*, **38**, 1989 (2004).

6. WHO, Unicef, Global Water Supply and Sanitation Assessment 2000 Report, Water Supply, 87 (2000).

7. F. Jin and H. Enomoto, *BioResources*, **4**, 704 (2009).

8. T. Karak and P. Bhattacharyya, *Resour. Conserv. Recycl.*, **55**, 400 (2011).

9. W. Qiao, W. Wang, X. Wan, Z. Xia and Z. Deng, *J. Residuals Sci. Technol.*, **7**, 7 (2010).

10. G. Langergraber and E. Muellegger, *Environ. Int.*, **31**, 433 (2005).

11. S. Deng, H. Tan, X. Wang, F. Yang, R. Cao, Z. Wang and R. Ruan, *Bioresour. Technol.*, **239**, 302 (2017).

12. T. Liu, Y. Guo, N. Peng, Q. Lang, Y. Xia, C. Gai and Z. Liu, *J. Anal. Appl. Pyrolysis*, **126**, 298 (2017).

13. M. Gong, W. Zhu, H. Zhang, Y. Su and Y. Fan, *J. Supercrit. Fluids*, **113**, 112 (2016).

14. H. Han, S. Hu, S. S. A. Syed-Hassan, Y. Xiao, Y. Wang, J. Xu, L. Jiang, S. Su and J. Xiang, *Bioresour. Technol.*, **236**, 138 (2017).

15. C. He, C. L. Chen, A. Giannis, Y. Yang and J. Y. Wang, *Renew. Sustain. Energy Rev.*, **39**, 1127 (2014).

16. T. Yanagida, T. Minowa, A. Nakamura, Y. Matsumura and Y. Noda, *J. Jpn. Inst. Energy*, **87**, 731 (2008).

17. S. Petzet, B. Peplinski and P. Cornel, *Water Res.*, **46**, 3769 (2012).

18. L. Qian, S. Wang and P. E. Savage, *Bioresour. Technol.*, **232**, 27 (2017).

19. L. Huan, J. Yiying, R. B. Mahar, W. Zhiyu and N. Yongfeng, *J. Hazard. Mater.*, **161**, 1421 (2009).

20. J. Diak, B. Örmeci and C. Proux, *Water Sci. Technol.*, **63**, 1309 (2011).

21. J. L. Urrea, M. García, S. Collado, P. Oulego and M. Díaz, *J. Environ. Manage.*, **206**, 284 (2018).

22. J. L. Urrea, S. Collado, A. Laca and M. Díaz, *J. Water Process Eng.*,

5, 153 (2015).

23. R. T. Haug, D. C. Stuckey, J. M. Gossett and P. L. Mccarty, *Water Pollut. Control Fed.*, **50**, 73 (1978).

24. Y. Wu, K. Song, Y. Jiang, X. Sun and L. Li, *Biochem. Eng. J.*, **139**, 132 (2018).

25. J. A. Rollin, Y. J. Bomble, P. C. St. John and A. K. Stark, *Biochem. Eng. J.*, in press (2018).

26. K. Cantrell, K. Ro, D. Mahajan, M. Anjom and P. G. Hunt, *Ind. Eng. Chem. Res.*, **46**, 8918 (2007).

27. M.-M. Titirici, A. Thomas and M. Antonietti, *New J. Chem.*, **31**, 787 (2007).

28. J. A. Libra, K. S. Ro, C. Kammann, A. Funke, N. D. Berge, Y. Neubauer, M.-M. Titirici, C. Fühner, O. Bens, J. Kern and K.-H. Emmerich, *Biofuels*, **2**, 89 (2011).

29. A. Kato and Y. Matsumura, *J. Jpn. Inst. Energy*, **82**, 97 (2003).

30. R. Matsumoto, T. Aki, Y. Okamura, T. Tajima, Y. Nakashimada and Y. Matsumura, *J. Jpn. Inst. Energy*, **93**, 531 (2014).

31. F. Yin, H. Chen, G. Xu, G. Wang and Y. Xu, *Bioresour. Technol.*, **198**, 351 (2015).

32. J. Moon, T. Y. Mun, W. Yang, U. Lee, J. Hwang, E. Jang and C. Choi, *Energy Convers. Manag.*, **103**, 401 (2015).

33. T. Yoshida, H. Nonaka and Y. Matsumura, *J. Jpn. Inst. Energy*, **84**, 544 (2005).

34. P. Petchpradab, T. Yoshida, T. Charinpanitkul and Y. Matsumura, *Ind. Eng. Chem. Res.*, **48**, 4587 (2009).

35. J. Yu, M. Guo, X. Xu and B. Guan, *Water Res.*, **50**, 10 (2014).

36. T. Kyotani, S. Hayashi and A. Tomita, *Energy Fuels*, **5**, 683 (1991).

37. L. Wang, A. Li and Y. Chang, *Water Res.*, **112**, 72 (2017).

38. D. C. Elliott, P. Biller, A. B. Ross, A. J. Schmidt and S. B. Jones, *Bioresour. Technol.*, **178**, 147 (2015).

39. U. Çolak, H. Durak and S. Genel, *J. Supercrit. Fluids*, **140**, 53 (2018).

40. The National Environmental Services Center, Pipeline, **14**, 1 (2003).

41. Y. Unami, M. Kanna, T. Yanagida and Y. Matsumura, Pa-216, In: Proc. 8th Conference on Biomass Science, Higashi-Hiroshima, Jan. 9-10, 2013, Higashi-Hiroshima, Japan (in Japanese).

42. J. G. Everett, *J. Water Pollut. Control. Fed.*, **44**, 92 (1972).

43. L. Wang, L. Zhang and A. Li, *Water Res.*, **65**, 85 (2014).

44. M. Imbierowicz and A. Chacuk, *Water Res.*, **46**, 5747 (2012).

45. R. Mohamad, T. Aki, Y. Nakashimada, Y. Okamura, T. Tajima and Y. Matsumura, *J. Japan Pet. Inst.*, **59**, 149 (2016).

46. M. Goto, T. Nada, A. Kodama and T. Hirose, *Ind. Eng. Chem. Res.*, **38**, 1863 (1999).

47. C. Bougrier, J. P. Delgenès and H. Carrère, *Chem. Eng. J.*, **139**, 236 (2008).